Research Article

Binding and Specificity of Ovalbumin with Chitosan Derivatives Varying in Degree of Acetylation

Irina L. Zhuravleva[1] , Evgeniya A. Bezrodnykh[2] , Victor N. Orlov[3] , Boris B. Berezin[2] , Vladimir E. Tikhonov[2] , Yurij A. Antonov[1*]

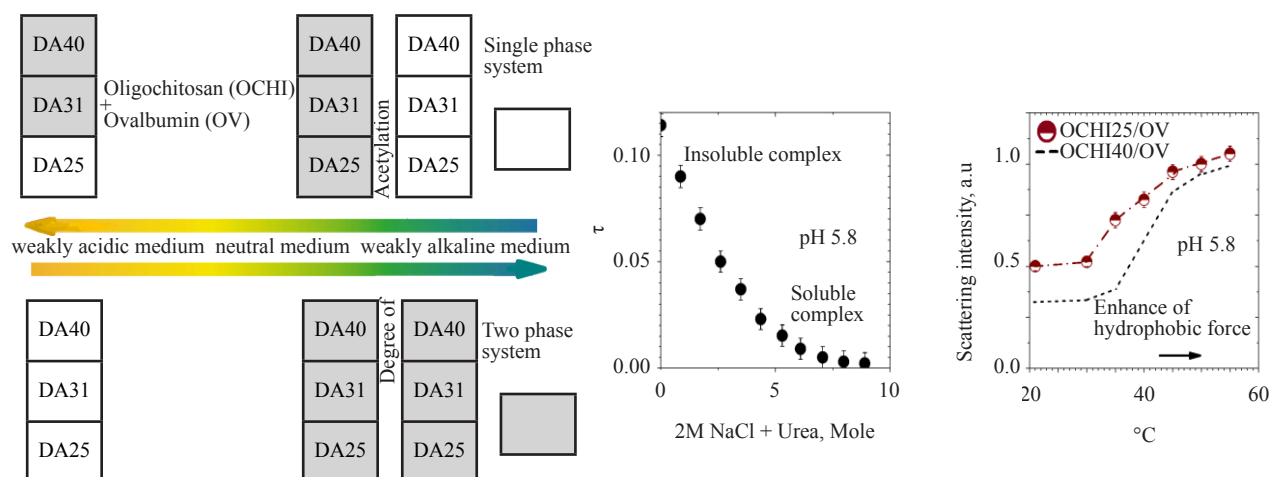[1]N. M. Emanuel Institute of Biochemical Physics, Russian Academy of Sciences, Moscow, Russia
[2]A. N. Nesmeyanov Institute of Organoelement Compounds, Russian Academy of Sciences, Moscow, Russia
[3]A. N. Belozersky Research Institute of Physico-Chemical Biology, Moscow State University, Moscow, Russia
 Email: chehonter@yandex.ru

Abstract: Here is an insight into the interaction and formation of insoluble complexes of ovalbumine (OV) with a series of specific chitosan derivatives (oligochitosan (OCHI)), varying in the degree of acetylation (DA) in acidic, neural and alkaline media. The forces involved in the complexation are determined and discussed. As shown, the interaction is partially electrostatic by nature with the "molar" composition in the insoluble OCHI-25/OV and OCHI-31/OV complexes of 1:2.8 and 1:2.1, respectively. The interaction is also partially hydrophobic and intensified at elevated temperatures. It is found that the binding of OV to OCHI and stability of the complexes depend on the way they are formed, and the affinity of OV to OCHI weakens with the increase in the DA. The complexes formed in a slightly acidic solution are limitedly soluble at a high solution ionic strength, and the aggregative state of the complexes depends on the weight fraction of OCHI in the complexes. The finding can be useful for understanding the complexation processes of chitosan with proteins and can be promising as a platform for the preparation of ovalbumin-based vaccines.

1. Introduction

Proteins as well as natural and modified polysaccharides are of great and increasing interest for usage in various fields of technology.[1,2] As has been shown, the mixing of protein and polysaccharide solutions can lead to segregative phase separation (also known as the limited thermodynamic compatibility, LTC) or associative phase separation (APS) accompanied by the formation of complex coacervates and insoluble complexes depending on experimental conditions (concentration, pH, ionic strength, surface charge). Two-phase systems of the first type (LTC) are widely used in food technology for protein processing into textured materials and in biotechnology for isolation, fractionation and purification of proteins.[3-6] The LTC has been observed and described for a vast majority of protein-polysaccharide mixtures at a sufficiently high critical concentration of biopolymers (> 1 ~ 3wt%). The condition of LTC manifestation corresponds to the absence of complexation between two biopolymers and the enhancement of protein self-association.[7]

An important feature of two-phase systems of the second type (ASP) is a significant improvement in the functional properties of both biopolymers. Another feature is that the phase separation takes place in dilute solutions (< 0.01 mg/ml), and is influenced by solution ionic strength and pH value.[8,9] For these reasons, two-phase protein-polysaccharide systems have found a wide application for tissue engineering[10], in the food industry, for improvement of functional properties of proteins[11,12], encapsulation and controlled drug delivery systems[13,14], in biotechnology for isolation, fractionation and purification of proteins[15,16] and immobilization and stabilization of enzymes in complexes.[17] As a result, the complexation in protein/polysaccharide systems is still under extensive study for many types of proteins and polysaccharides and is reviewed several articles and books.[4,18-21] However, there is a limited number of studies on the influence of the local structural changes in the polysaccharide (number of charged and uncharged groups, their distribution along the chain, etc.) on the complexation. The data published on this topic relate exclusively to pectin/beta-lactoglobulin[22,23] and pectin/lysozyme systems.[24-26] In general, local structural changes can significantly alter the charge density of the polysaccharide and the stiffness of its chains as well as being able to have an impact on the protein/polysaccharide complexation. Therefore, studies in this field would be very important for the use of protein/polysaccharide systems in various fields of technology.

Chitosan has found a wide application in the food industry and pharmaceuticals due to its polyelectrolyte nature, biodegradability and nontoxicity.[27,28] As a cationic polyaminosaccharide, chitosan can form complexes with other globular proteins including OV in solution whose properties depend on their composition.[29,30] The complexation of OV with chitosan leads to the stabilization of OV fibrils and helps to encapsulate bioactive nutrients increasing their stability and controlled release in the intestinal.[31-36] So far, only one study has been carried out on the effect of the molecular weight of chitosan (15, 100 and 200 kDa) on its interaction with BSA.[37] It has been shown that the three chitosan samples interact with BSA to form chitosan-BSA complexes with the affinity order: 200 > 100 > 15 kDa. The influence of another structural parameter of chitosan, namely the degree of acetylation (DA) on its complexation with proteins, has not yet been studied. Therefore, the interaction and the binding forces as well as conditions behind the formation of complexes between ovalbumin (OV) and chitosan differing in the DA, which are important to the food and medical fields, still remain unclear and need to be studied.

It is well known that natural chitin is insoluble in diluted organic (acetic and lactic) or inorganic (hydrochloric) acids.[38] When the degree of deacetylation of chitin reaches the value of 60% and more, chitin becomes soluble in diluted acetic or hydrochloric acids and it is called "chitosan". As shown and discussed in several articles, chitosan could be distinguished from oligochitosan (short-chain chitosan) by molecular weight (MW). The term "oligochitosan" (OCHI) can be used for chitosan molecules with molecular weight (MW) ≤ 16 kDa (or degree of polymerization: n ≤ 100).[39-41] As has been shown, OCHI has several advantages over chitosan since OCHI possesses a higher solubility, lower solution viscosity, increased antimicrobial activity and enhanced oral and mucosal adhesion.[42-46] Moreover, light scattering and microscopy studies have shown that OCHI having MW ≤ 12 kDa and DA 16 ~ 35% can be considered as a specific group of chitosan derivatives with a peculiar high stability of their solutions in alkaline media [47] Unfortunately, the complexation of OV with specifically acetylated OCHI has not been studied so far despite chitosan/OV complex microparticles being promising as immunomodulators and adjuvants.[48] The lack of experimental data has moved us to study the impact of the changes in the degree of OCHI acetylation on the interaction and binding with OV in semi-

diluted solution using a series of OCHI derivatives varying in the degree of acetylation in acidic, neutral and alkaline media.

In this study, we aimed to gain an insight into the interactions and the forces as well as conditions responsible for the formation of complexes between ovalbumin (OV) and OCHI samples differing in the degree of acetylation (DA) from 25% to 40% at varying and constant pH conditions.

2. Materials and methods

2.1 *Materials*

Ovalbumin (purity > 98%, isoelectric point IEP 4.8, molecular weight: 45 kDa) was purchased from Sigma Co. (St. Louis, MO); sodium acetate, sodium chloride, hydrochloric and acetic acids were the products of Merck.

Oligochitosan hydrochloride samples (OCHI-25, OCHI-28, OCHI-31, and OCHI-40) with the weight average molecular weight M_w 12 ± 0.5 kDa and DA 25, 28, 31, and 40% were prepared by N-reacetylation of oligochitosan with the weight average molecular weight M_w 11.9 kDa and DA 2% following the next protocol.[47] The DA values were determined by ^{1}H-NMR and recorded at 25 °C.[57]

Stock solutions of OV and OCHI were prepared in 10 mM sodium acetate/acetic acid buffer (pH 5.8) with ionic strength I = 0.01 and centrifuged to remove insoluble matter. Biopolymer concentration in stock solution was determined by measuring the drying at 104 °C until a constant weight. Complex OCHI/OV systems with different OCHI/OV weight ratios (q) were prepared by adding of OCHI solution drop-by-drop to OV solution at 23 °C.

2.2 *Methods*

2.2.1 *Turbidity measurements*

The turbidity value (τ) of the OCHI/OV complex system as a function of q (wt./wt.) was determined at 500 nm. The error of measurements was about 2%-3% at 500 nm. The main complexation parameters: q_{Onset}, q_ϕ, q_{Max}, and q_{Set}, (where: q_{Onset} and q_{Set} are the values indicating the transitions between no complex formation and the formation of soluble complexes, q_ϕ indicating the transition between the formation of soluble and insoluble complexes, and q_{Max} indicating the q ratio that corresponded to a maximum of system turbidity) were determined following the method offered by Antonov et al.[24] To determine accurately the values of transition points, additional characterizations were performed. The q_{Onset} value was determined by turbidimetric titration as indicated below in Figure 3d. These results were confirmed by dynamic light scattering (DLS) data in which the average size of the complexes exceeded that of OV by 10%. The q_{Set} value was the minimum q value at which the turbidity value of the OCHI/OV mixture became equal to that of the OCHI solution with the same OCHI concentration as in the mixture. The q_ϕ values were determined as the minimal q values at which turbidity increased with the time, which was quantified as an increase of > 2% during 15 min under quiescent conditions for samples that had been stirred for 30 min before the test.

2.2.2 *Dynamic light scattering (DLS) and electrophoretic mobility*

Particle size distribution functions were obtained using a Malvern Zetasizer Nano-ZS (England) as shown earlier.[24] The ς-potentials at different q values and pH were measured at 23 °C, and the average value of ten measurements was shown.

2.2.3 *Brightfield imaging*

Microscopy images were made using a multi-beam confocal microscope Leica TSC SP-5.

3. Results and discussion

3.1 *Phase behavior of OCHI/OV systems*

3.1.1 *Effect of pH and formation pathway on complexation*

Two biopolymers effectively form electrostatic and insoluble complexes in an aqueous solution, usually when biopolymers are charged oppositely and the values of the charges provide mutual compensation.[5,19] Therefore, the method of turbidimetric titration of protein/polysaccharide mixtures from an alkaline pH region to an acidic region, or *vice versa*, is widely used to study the phase behavior of mixed biopolymer systems.[29,49,50]
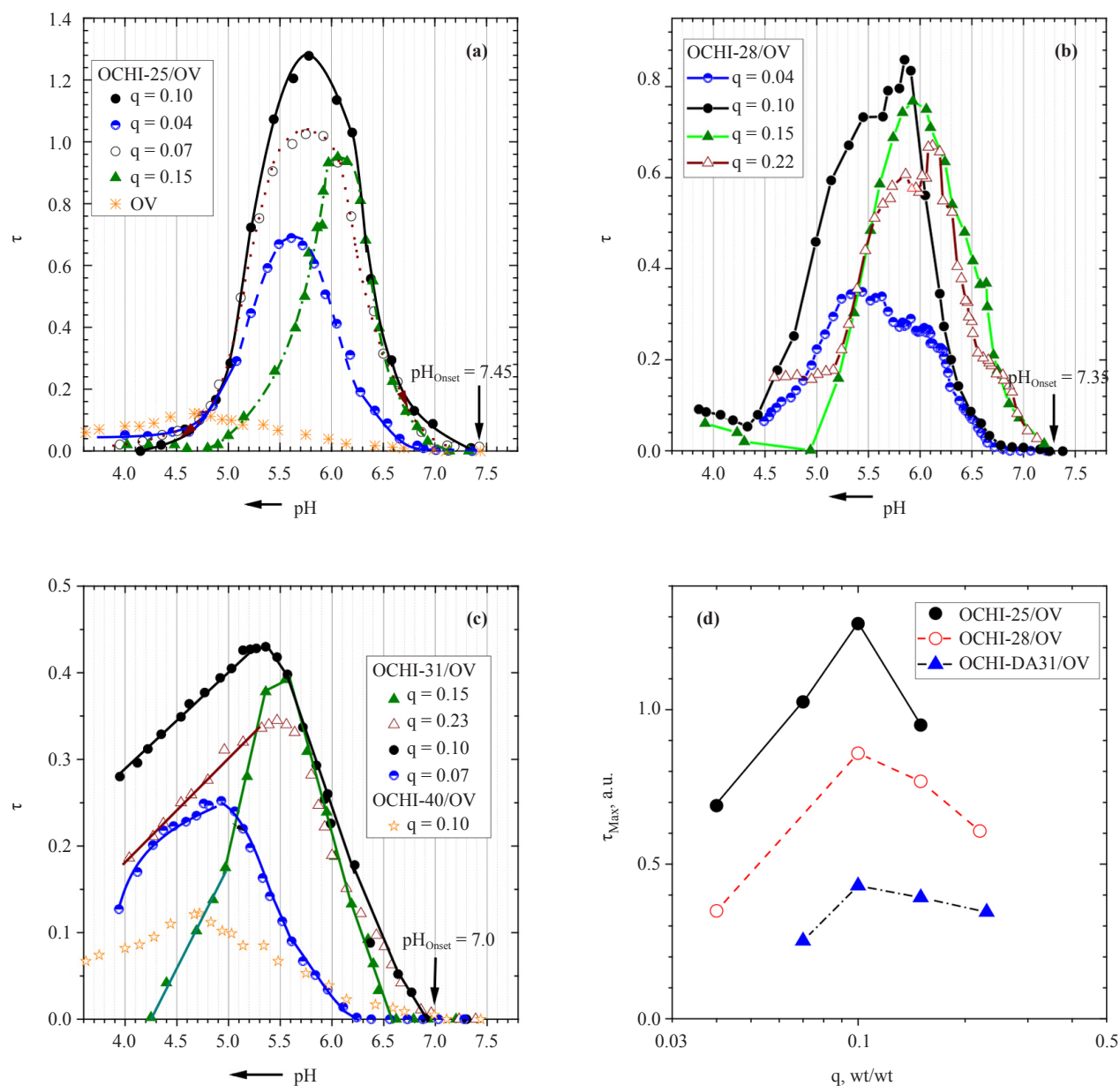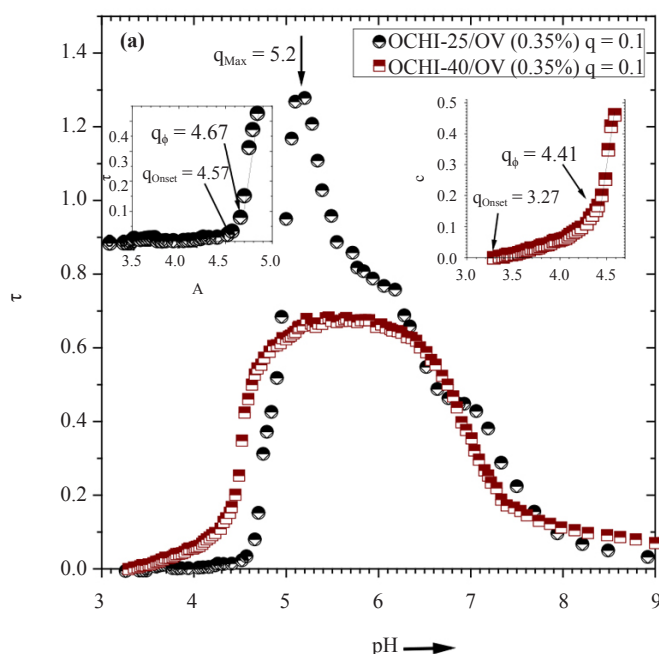

Figure 1. Turbidity curves of OCHI/OV mixtures as a function of pH at various q values and the OV concentration in mixture 0.35wt%: (a) OCHI-25/OV, (b) OCHI-28/OV, (c) OCHI-31/OV and OCHI-40/OV mixtures, (d) maximum turbidity (τ_{Max}) of OCHI/OV system as a function of *q* at *I* = 0.01 and 23 °C. The arrow shows the titration pathway
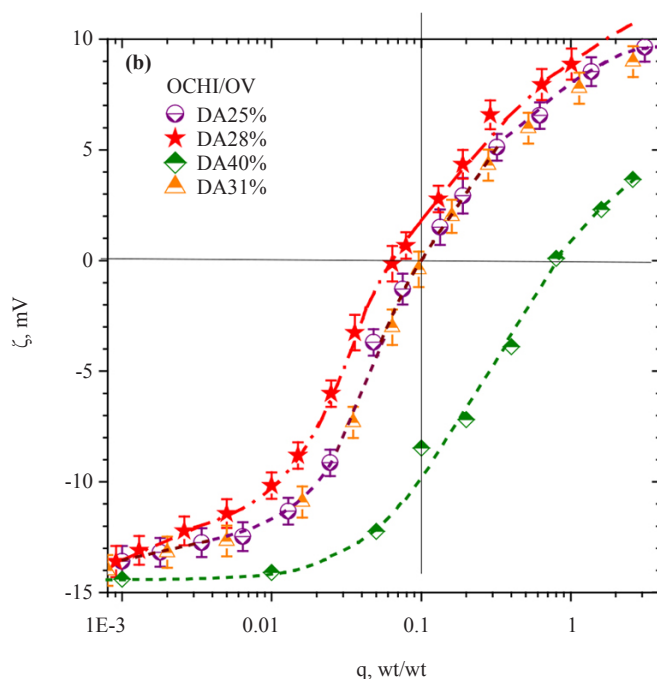
Figure 1 shows the curves of pH titration of OCHI/OV systems starting from alkalescent (pH 7.5) to acidic region (pH 4.0), i.e. at pH region in which OCHIs are completely soluble. As shown in Figure 1, the turbidity of pure OV solution at pH < 6.1 increases slightly due to a self-aggregation of the protein molecules and reaches the maximum value at pH 4.75 (isoelectric point of OV).

A decrease in pH is accompanied by an increase in the turbidity (τ) of mixtures at all q values studied and depends on the DA of OCHI. The dependences have an extreme character with the maximum (q_{Max}) corresponding to the maximal yield of the insoluble complexes. As shown in Figures 1a-c for systems containing OCHI with DA 25%, 28% and 31%, the maximal turbidity (and consequently the maximal size and/or yield of OCHI/OV complexes) occurs in the range of q values equal to ~0.10 and decreases with an increase in DA values (Figure 1d). The critical pH_{Onset} value above which complexes do not form decreases noticeably (from pH 7.45 to pH 7.0) with an increase in DA values of OCHI.

Complexes obtained by titration of a biopolymer mixture with alkali or acid from the region of the single-phase state of the system to the two-phase state region are defined as "complexes of titration". Such complexes may be non-equilibrium, and their composition can depend on the way of their formation.[51,52] To verify or refute the influence of the pathway, the titration of OCHI/OV systems from the acidic region to a slightly alkaline region was carried out. The corresponding data of OCHI-25/OV and OCHI-40/OV systems are presented in Figure 2. As shown, conditions of formation and dissociation of insoluble complexes as well as their stoichiometric composition strongly depend on the pathway of the preparation.

Complexes of titration of OCHI-25/OV system from the alkalescent to acidic region start to form at pH less than 7.1 ~ 7.4 while complexes of the same system obtained by titration from the acidic pH region to the slightly alkaline region are present in the mixture and at higher pH values. (Figure 2a). A similar phenomenon is observed for the OCHI-40/OV system. The pH_{Max} value corresponding to the maximal turbidity of the system, that is the maximum of the complexation, occurs at pH 5.2 when the titration from the acidic to the alkalescent region is carried out. In contrast, when the titration of the mixture is carried out from the alkalescent region to the acidic region the maximal turbidity occurs at $pH_{Max} = 5.8$.

Figure 2. (a) Turbidity curves of OCHI/OV mixtures as a function of pH at q values equal 0.10 and OV concentration in mixture of 0.35wt%: $I = 0.01$, 23 °C. The arrow shows the titration from acidic to alkalescent region, (b) average zeta potentials of OCHI/OV system as a function q at OV concentration in the mixture of 0.35wt% and at $I = 0.01$ and 23 °C

Likewise, this pathway dependence was characteristic of OCHI-40/OV system. When the system was titrated from a slightly alkaline to an acidic region, complexes were not formed at pH values > 6.9. In contrast, insoluble complexes were observed at the reverse titration of the system even at pH = 9.0 with pH_{Max} value, which was similar to that observed for the OCHI-25/OV system (pH 5.2), but the formation of insoluble complexes was observed over the wider range of pH values from pH 5.2 to pH 6.0. The pH_{Onset} values for OCHI-25/OV and OCHI-40/OV systems during the titration to the alkalescent region were 4.57 and 3.27, respectively, and the q_ϕ values characterizing the system transition from a single-phase to the two-phase state were found to be 4.67 and 4.41, respectively.

The results of the turbidimetric titration indicate that conditions required for the formation and dissociation of the insoluble complexes depend on the pathway of preparation. Moreover, the stoichiometric composition of such complexes would likely differ at a lower relative content of OCHI in the mixture from the composition of the complexes obtained by titration of the mixture from alkalescent to the acidic region with the composition containing a lower quantity of OCHI in the complex. To conclude this section, it should be noted that the nonequilibrium of system titration complexes indicates the need to study complex formation processes under conditions of constant pH value of the solutions and their mixtures.

3.1.2 *Zeta potentials of OCHI, OV and OCHI/OV systems and the main parameters of complexation at pH 5.8*

In a buffer solution with pH 5.8, the ς-potential of OV was equal to -14.3 ± 07 mV which was close to the earlier published data.[53] Electrophoretic study of the surface charges of OCHI solutions showed that their zeta potentials altered non-linearly with the degree of acetylation and were of +17.7 ± 1.5 mV, 15.8 ± 1.8 mV, 15.5 ± 1.6 mV and 10.3 ± 2.7 mV for OCHI-25, OCHI-28, OCHI-31, and OCHI-40, respectively. Therefore, these biopolymers had opposite charges required for electrostatic interaction. To determine the effective surface charge of OCH/OV complexes, their zeta potentials were measured.

Figure 2b shows the dependence of the zeta potentials of OCHI/OV systems as a function of the OCHI/OV weight ratio (q) depending on the DA value of OCHI. As shown, the negative charge of OV neutralizes rapidly upon the association of OV with OCHI, and the surface charge of the formed complexes becomes positive at higher q ratios. It is

noteworthy that the change in the zeta potential of the OCHI-40/OV system is significantly different from that in other systems containing OCHI-25, OCHI-28, and OCHI-31. Unlike the last three systems where the zeta potentials reach the zero value at q = 0.10-0.13, the value of the zeta potential of OCHI-40/OV complexes becomes equal to zero at a significantly higher value of q that is 0.8, which can be related to a lower total charge of OCHI due to its higher DA value.

To investigate the structure of the OCHI/OV complex phase, complexation parameters characterizing the aggregation and phase separation were quantitatively determined. The mixing of OV and OCHI solutions led to a fast solution turbidity when OCHI/OV weight ratio (q) exceeded the q_{Onset} value.
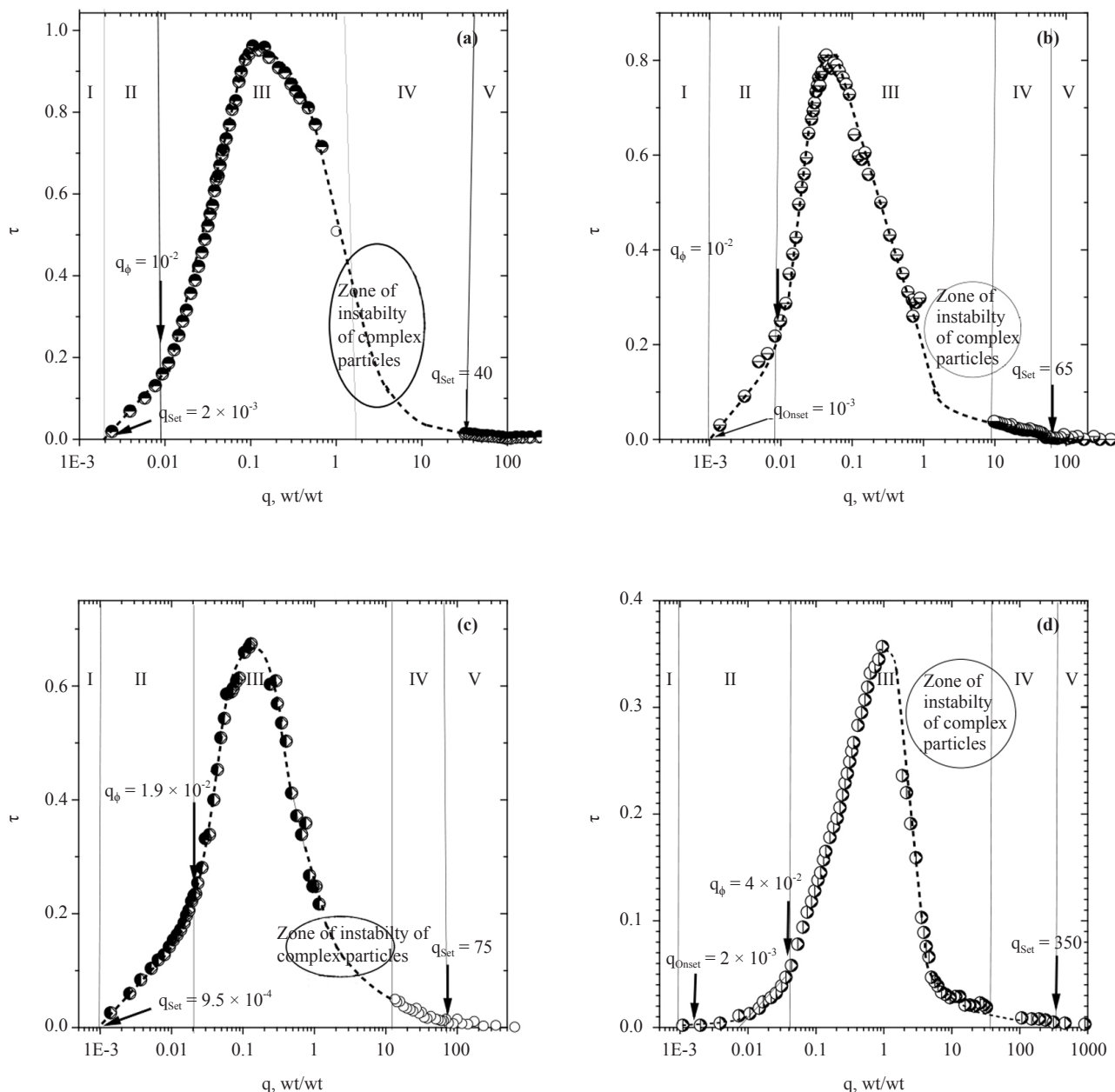

Figure 3. The turbidity values (τ) as a function of the OCHI/OV weight ratio q for OCHI-25/OV (a), OCHI-28/OV (b) OCHI-31/OV (c) and OCHI-40/OV (d) mixtures at I = 0.01, pH 5.8, 23°C and C^M_{OV} = 0.20 wt.%

Figure 3 shows turbidity values (τ) as a function of q of OCHI/OV complex systems based on OCHI-25, OCHI-28, OCHI-31, and OCHI-40. Using the turbidity as a function of q, transitions in OCHI/OV mixed system between miscible, soluble complex, and insoluble complex can be pinpointed (Figures 3a-d, region I-V). As shown, turbidity of OCHI/OV mixture depends on DA and q values, and consequently, on the charge ratio of two biopolymers in the complex. Thus, the dependence of τ on q has an extremal character with the maximum observed at $q_{Max} = 0.10$ for OCHI-25 systems, $q_{Max} = 0.045$ for OCHI-28/OV system, $q_{Max} = 0.13$ for OCHI-31/OV system and $q_{Max} = 0.90$ for OCHI-40/OV system, respectively. The τ_{Max} value is maximal for the system containing the most charged OCHI-25, and it is minimal for the system containing the lesser charged OCHI-40. As it follows from turbidity data, it seems that the electrostatic interaction of oppositely charged OV and OCHI macroions plays an important role in the complexation of these biopolymers. As OV has MW = 45 kDa[54] with that of OCHI being on average 12 kDa, it is possible to approximately calculate the "molar" ratio OCHI/OV in the complex phase. A simple calculation can show that this ratio is ~1:2.8 mole OCHI/mole OV for OCHI-25/OV systems, and ~1:2 for OCHI-31/OV systems. Unexpectedly, the molar ratio of OCHI-28/OV in the complex phase is significantly different from those determined for two previous systems (1:6) mole OCHI-28/mole OV. The q_{onset} values for all the systems studied are small enough and close to each other in value ($1 \sim 2 \times 10^{-3}$). The value q_ϕ corresponding to the phase transition equal to $q_\phi = 10^{-2}$ for OCHI systems with DA 25% and DA 28% increases with further increase in DA to 31% and 40% by two-fold and four-fold, respectively.

3.1.3 *DLS studies, morphology and aggregate state of the complex phase*

DLS studies were carried out to determine the complex particle sizes at different q values. The results of the measurements are presented in Figure 4a-f.
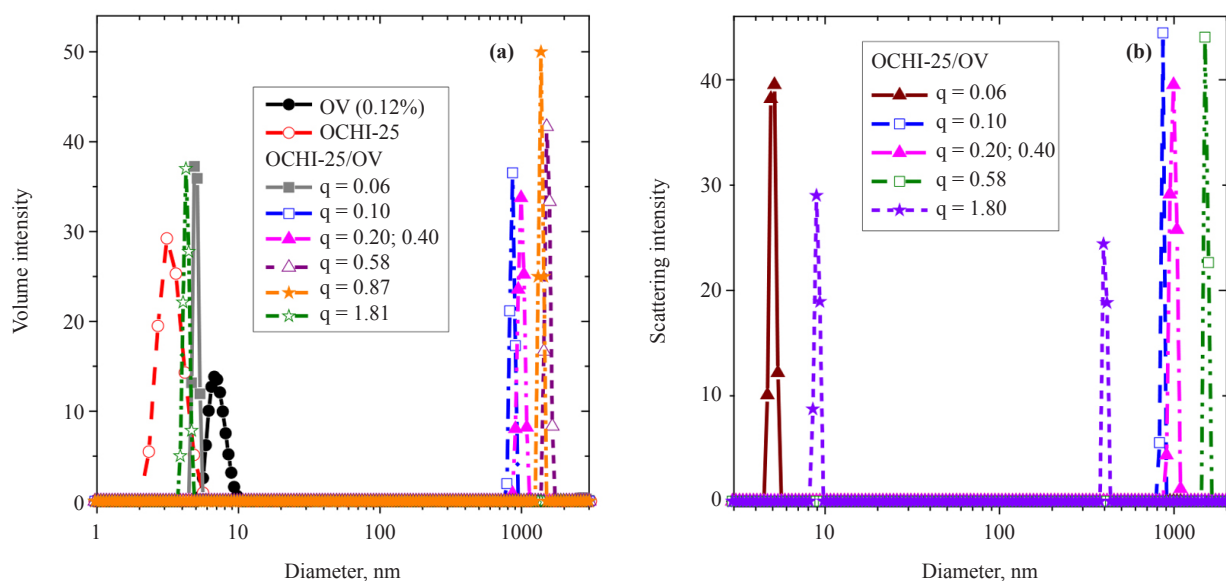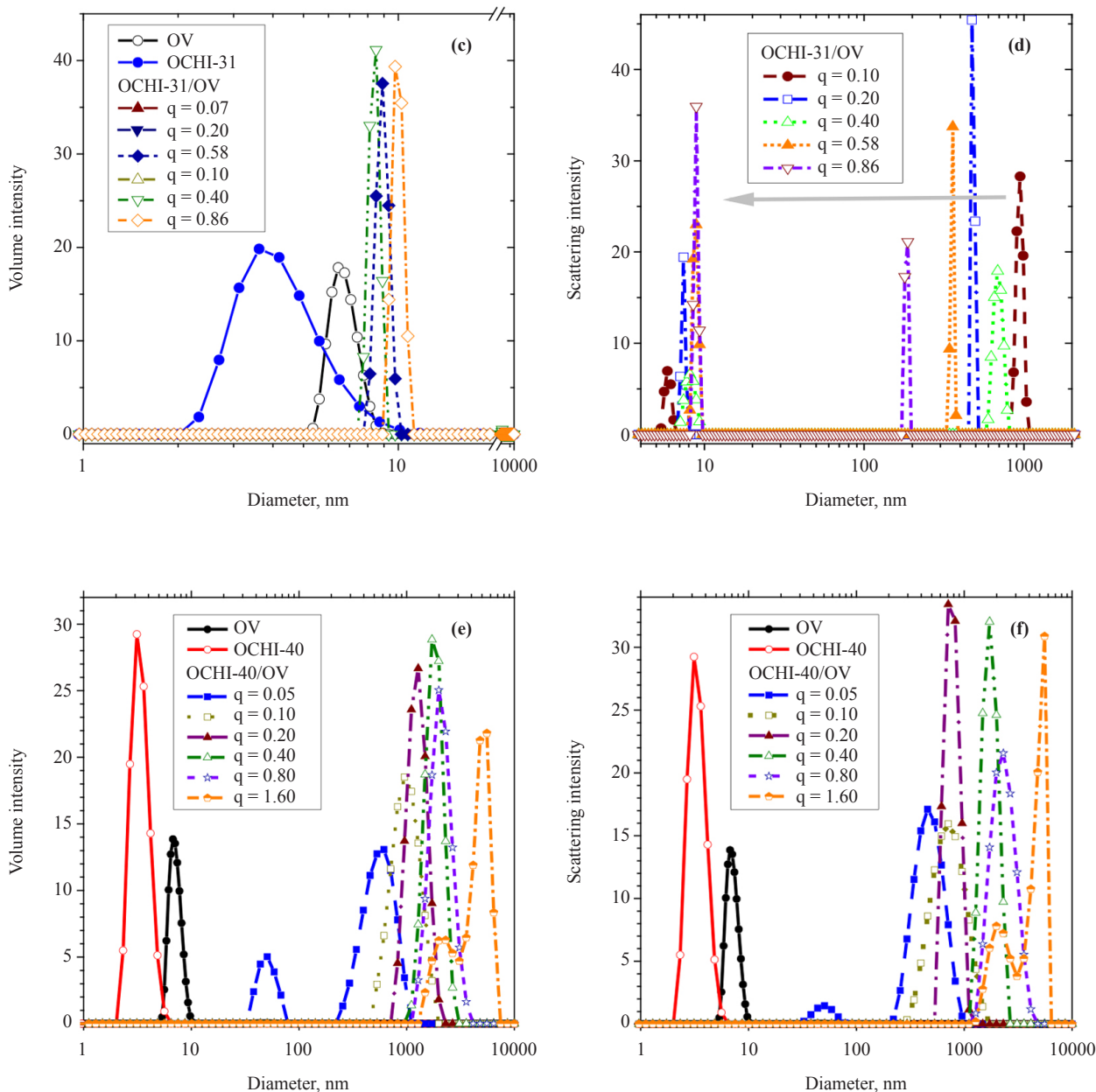
Figure 4. The intensity size distribution and volume size distribution as functions of q: (a, b) OCHI-25/OV system; (c, d) OCHI-31/OV system; (e, f) OCHI-40/OV system. The concentration of OV in mixtures 0.10 wt.% at pH 5.8, $I = 0.01$, 23 °C

The measurements were performed at a constant OV concentration (0.1 wt.%) over a wide range of q values from 0.06 to 1.80. The average sizes of OCHI and OV molecules were of ~3.6 nm and ~6.5 nm, respectively (Figure 4b). As shown in Figure 3a, the interaction of OV with OCHI-25 at $q = 0.10$ (q_{Max}) corresponding to both the stoichiometric composition of the system and zero value of zeta potential (Figure 2 b) resulted in the formation of insoluble complexes with the average size of 850 nm that increased up to 1,300 nm at $q = 0.87$. A further increase in the weight ratio of OCHI-25 in the mixture led to a significant decrease in the size of complex particles since complex particles become positively charged at an excess of OCHI-25. Moreover, the average particle size dropped almost to that of the original size of the biopolymers at $q = 1.80$ (Figure 4b). The average particle size altered with increasing q in the OCHI-28/ OV system in the same sequence (data not shown). At increasing q, the change in the particle size of OCHI-31/OV and

OCHI-40/OV systems showed significant differences. First of all, the formation of soluble complexes was observed for both these systems at relatively low q values (Figure 4c-f), which were not observed for the systems containing OCHI-25 and OCHI-28. At $q \geq q_{Max}$, the OCHI-40/OV system formed complex particles with an average size that exceeded the limit of the measurements (6 μm). The results of DLS measurement of particle sizes depending on DA value and the weight fraction of OCHI (q) in the mixture with OV showed a significant role of secondary physical bonds in the formation and aggregation of complexes.
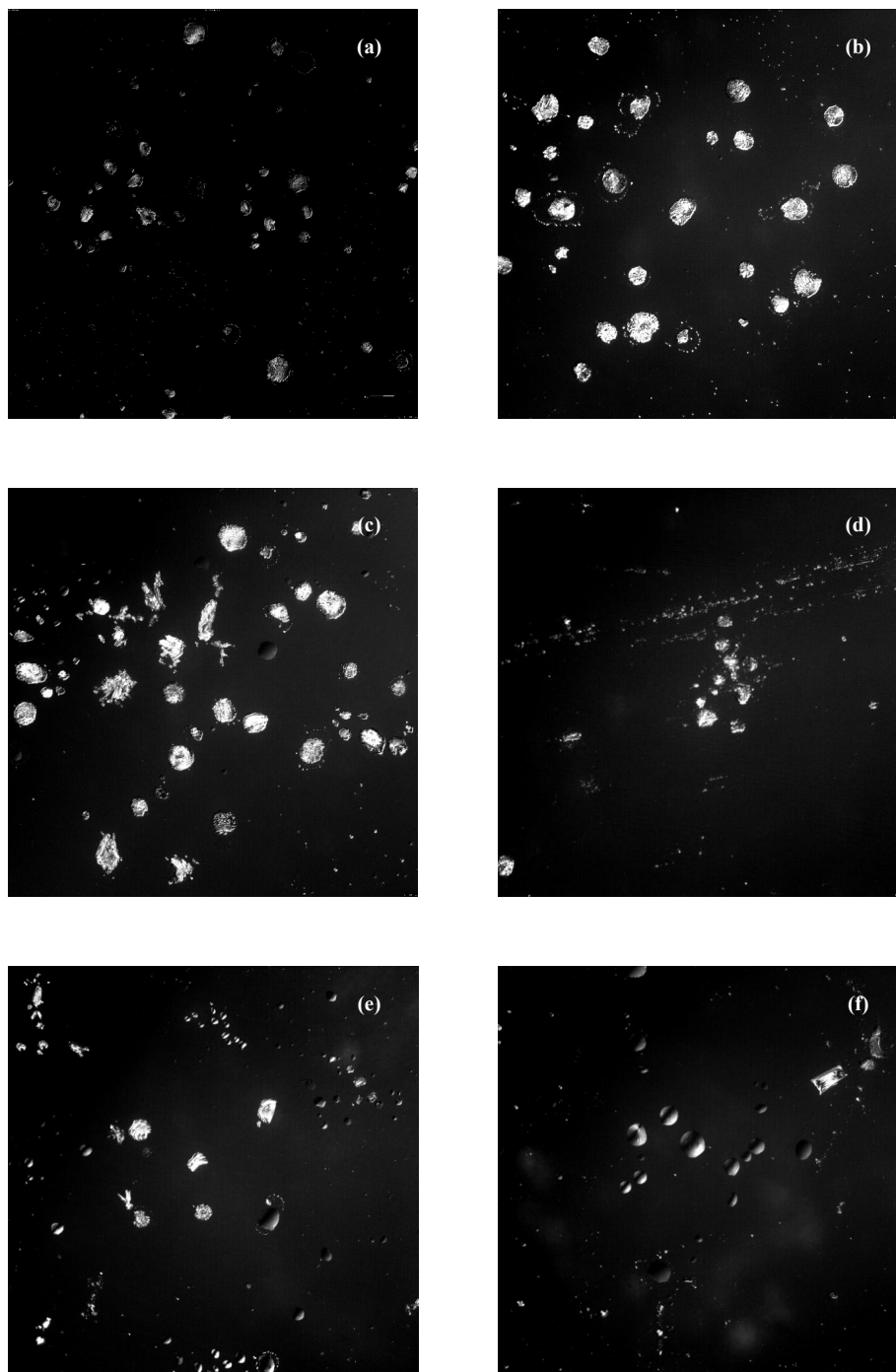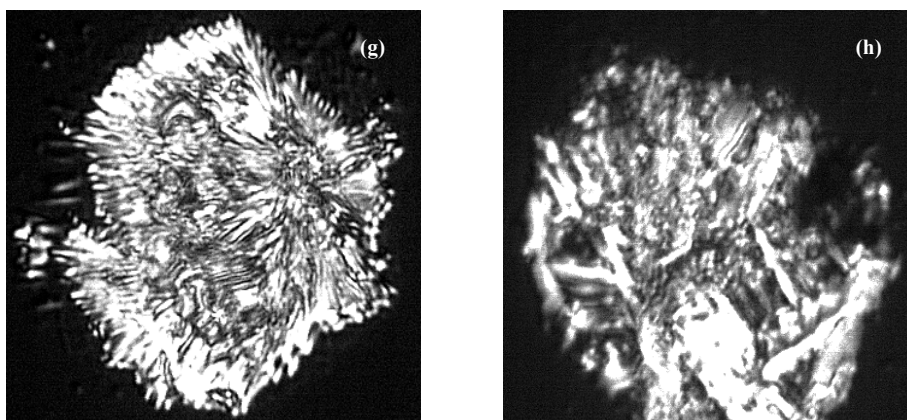
Figure 5. Bright field microscopy images of OCHI-25/OV systems at different q values: (a) $q = 0.07$; (b) $q = 0.10$; (c) $q = 0.20$; (d) $q = 0.40$; (e) $q = 0.58$; f) $q = 0.86$. The concentration of OV in the mixture $C^m_{OV} = 0.35$ wt./%. Full length of images is 730 μm. pH 5.8, $I = 0.01$, 23 °C; (g, h) complex particles for OCHI-25/OV systems (g) $q = 0.20$, (h) $q = 0.58$. Full length of images is 40 μm.

Bright field microscopy was used for visualization of OCHI-25/OV complex systems at different q values with the images being shown in Figure 5. At q ranged from $q = 0.07$ to $q = 0.40$, solid complex particles were slightly asymmetric in shape and had a pronounced internal structure (Figure 5a-d). Their average dimension ranged from 20 μm to 40 μm being slightly dependent on the relative content of OCHI in the mixture. With an increase in q up to $q = 0.58$ and further to $q = 0.86$, complex particles formed liquid droplets and the complex phase altered its state from solid to liquid. (Figure 5g-h).

In other words, a phenomenon of complex coacervation is observed. It should be noted that complex coacervation is usually observed in systems composed of proteins and weak polyelectrolytes, like Arabic gum[18] and pectin.[55] The transition from solid complex particles to coacervates is caused presumably by a decrease in the overall charge of pectin that significantly suppresses the interaction leading to an increased molecular mobility in the complexes apparently because of a difference in the conformation of molecules.[55,56] However, in our case, there is no drop in the surface charge at $q = 0.86$ compared to the system at $q = 0.20$ (Figure 2b). It can be assumed that the transition of complex phase from the solid to liquid state is caused by a significant alteration in the structure of OV due to an excess of OCHI in the system. The start of this transition can be traced from two images of the particles of the complex phase at $q = 0.20$ and $q = 0.58$ (Figure 5g-h). At $q = 0.20$, the complex particle has a well-developed mesh structure, while the mesh structure is already disorganized into an amorphous structure at $q = 0.58$.

Microscopy images of the complex OCHI-31/OV system at different q values were similar to those observed for the OCHI-25/OV system. The transition from solid complex particles to coacervates was observed at $q \geq 0.60$ (data not shown).

3.2 *Effect of ionic strength, urea and temperature on the complexation*

The contributions of Coulomb, hydrogen bonding and hydrophobic forces responsible for the interaction between OV and OCHI and the formation of OCHI/OV complex particles were evaluated by measuring OCHI/OV systems turbidity and light scattering intensity of mixed OCHI/OV systems at different q values and varied NaCl and/or urea concentrations. The effect of increased temperature on the interaction was studied as well. Figure 6a demonstrates the effect of solution ionic strength on the turbidity values of the systems.

As shown, an increase in ionic strength led to a decrease in the turbidity of all systems containing OCHI with DA from 25 to 40%. The turbidity values fell by half already at $I = 0.1$ for most systems except the OCHI-40/OV system. In the latter system, the fall occurred at $I = 0.35$. Above $I = 0.52$, a further increase of the ionic strength did not affect the turbidity that remained within $\tau = 20$-40% of the initial value at $I = 0.01$ even at an extremely high ionic force ($I > 2$).
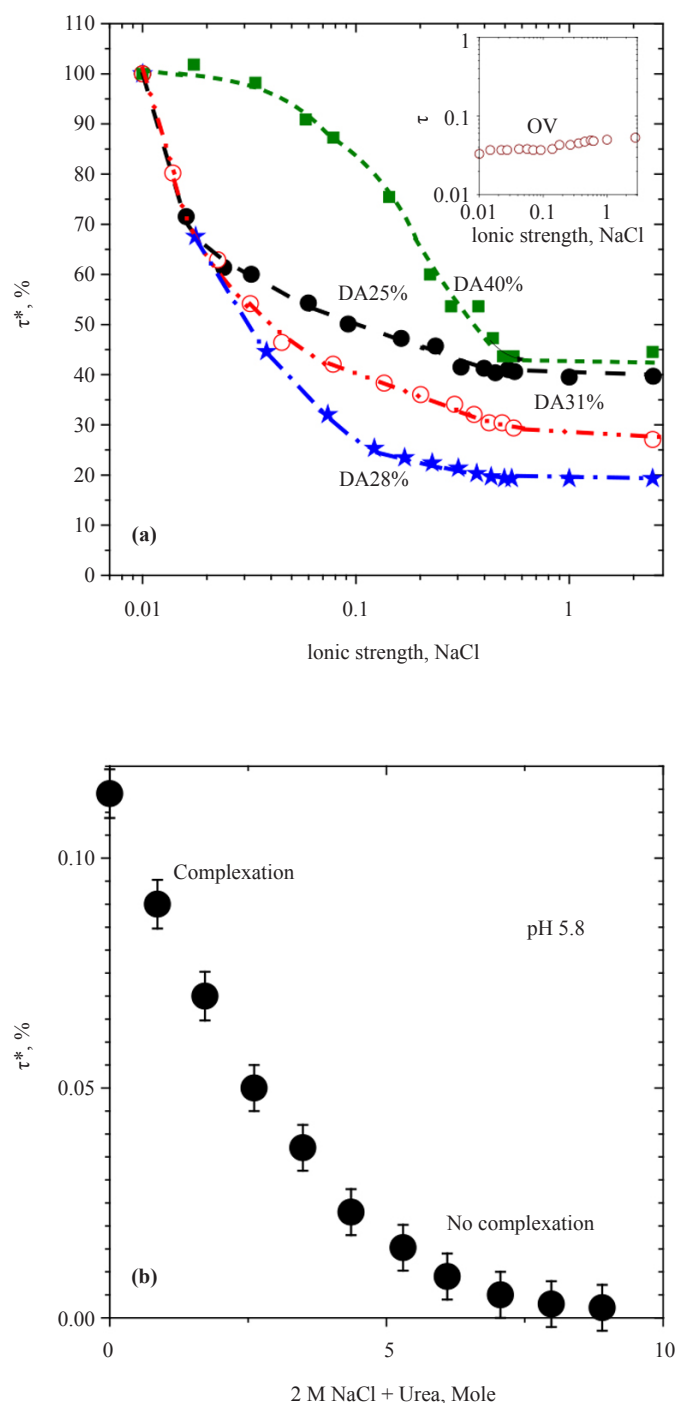
Figure 6. (a) Turbidity of OCHI-25/OV, OCHI-28/OV, OCHI-31/OV and OCHI-40/OV systems as functions of ionic strength at pH 5.8 and 23 °C. The turbidity values at $I = 0.01$ were taken as 100%. (b) Turbidity value of OCHI-40/OV system in the presence of 2 M NaCl as a function of the molar concentration of urea at pH 5.8 and 23 °C

It is important to note that the turbidity of the free OV solution is almost independent of the solution ionic strength up to $I = 2.0$ (insert in Figure 6a). This is not typical of conventional complexation usually occurring in protein/polyelectrolyte systems. It should be mentioned here that electrostatic interaction between biopolymers in most complex-forming protein/polysaccharide systems is usually suppressed at the ionic force equal to $I = 0.5$[16,24,55,56], i.e. at

the same *I* values as in OCHI/OV systems. Taking into account that the further increase in the ionic strength does not affect the turbidity of OCHI/OV systems regardless of the degree of OCHI acetylation, it becomes clear that electrostatic forces affect the complexation and stability of complexes in OCHI/OV systems only partially. Such complexes are also stabilized by secondary physical interactions (hydrophobic interactions and/or hydrogen bonds). This conclusion is confirmed by the data of turbidimetric titration of OCHI-40/OV/2 M NaCl system with urea at pH 5.8 (Figure 6b).

It is well known that the presence of 6-8 M urea in protein solution completely suppresses both hydrophobic interactions and the formation of hydrogen bonds. Figure 6b shows that as the concentration of urea increases the turbidity of the system decreases significantly, and the system becomes practically transparent at 8 M concentration of urea.

To assess the relative contribution of hydrophobic interactions and hydrogen bonds to the complexation, the effect of temperature on the light scattering intensity and particle size of OCHI-28/OV and OCHI-40/OV systems was examined (Figure 7a-b). It is necessary to mention that the systems should be stable during the examination and no sedimentation should occur during the heating and analysis to receive reliable results. To fulfill the requirements, the scattering measurements were carried out using supernatants of the complex systems.
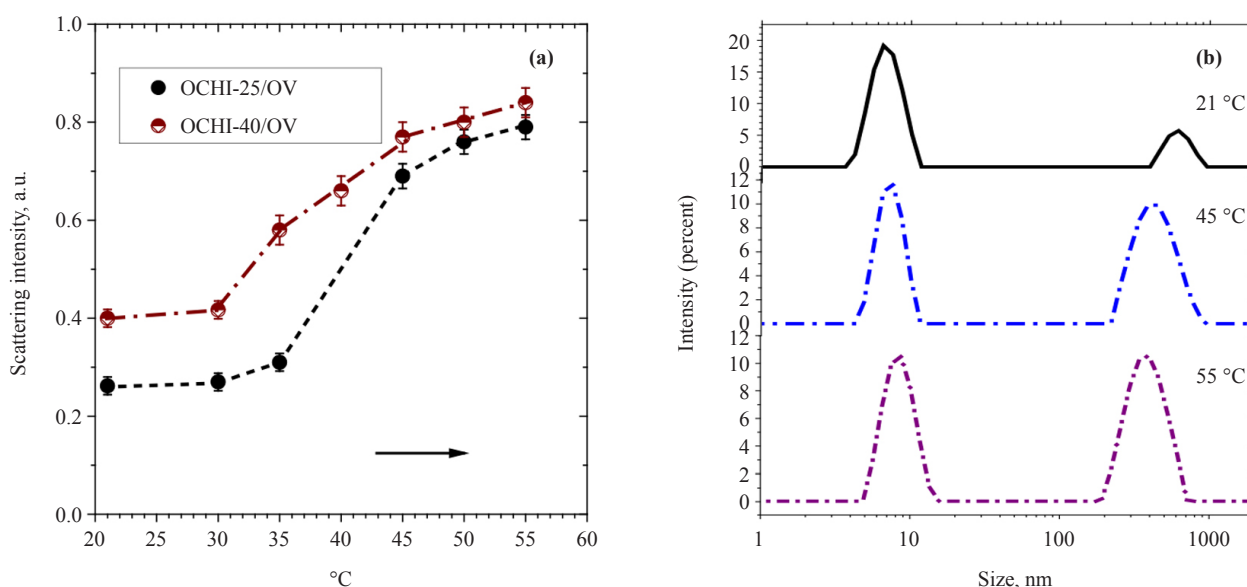
Figure 7. (a) Scattering intensity of supernatant of the OCHI-25/OV(0.25wt%) and OCHI-40/OV (0.25wt%) systems at q = 0.10 as a function of temperature at pH 5.8, I = 0.01; (b) Intensity size distribution function of supernatant of OCHI-25/OV(0.25wt%) system at different temperature and pH 5.8, I = 0.01

As shown in Figure 7a, a noticeable increase in the light scattering occurs when the temperature increases from 35 to 55 °C. Taking into account that the scattering values of both OV and OCHI solutions are not sensitive and remain intact in this temperature region. It can be assumed that the complexation of OV with OCHI is enhanced with an increase in temperature. The data on the particle size distributions at different temperatures shown in Figure 7b indicate both an increase in the interaction when the temperature rises from 30 °C to 55 °C and an increase in the quantity of complex particles with the average size of 400 nm. These data also demonstrate the impact of hydrophobic interaction on the complexation of OCHI with OV. In its turn, an increase in temperature has an inessential influence on the scattering of the system thus demonstrating a lower impact of hydrogen bonding on the complexation.

As a result, it can be assumed that the molecular mechanism of the complexation consists of the association of the oppositely charged OV and OCHI molecules together by electrostatic interaction with the formation of ion pairs between positively charged amino groups of OCHI and negatively charged carboxyl groups of aspartic and glutamic acids of OV. This interaction leads to the formation of neutral complex nanoparticles followed by a slow rearrangement

of these particles and the formation of insoluble complexes stabilized by secondary physical forces.

4. Conclusions

A series of specifically acetylated OCHI samples soluble both in acidic and alkaline solutions are prepared and used to investigate the main features of their interaction and binding with OV. It is found that the binding of OV to OCHI and stability of the complexes formed by titration of the systems from the acidic region to the alkaline one and the opposite way round differ. At constant pH 5.8, electrostatic binding of OV with OCHI-40 considerably decreases and reaches a maximum at a significantly higher OCHI/OV weight ratio ($q = 0.95$) compared with that of OCHI-25 and OCHI-31 ($q = 0.10 \sim 0.13$). At different experimental conditions (medium pH and ionic strength, thermal regime), an exceptional role of hydrophobic interactions in stabilizing insoluble complexes containing OCHI-40 is found. In contrast to ovalbumin/chitosan complexes described earlier, this new knowledge about the interaction of ovalbumin with new chitosan derivatives represents an important contribution to the preparation of ovalbumin/chitosan complexes which can find application for the construction of drug delivery systems.

Acknowledgments

Credit authorship contribution statement

I. L. Zhuravleva: methodology, spectroscopy analysis; E. A. Bezrodnykh: chemical methodology, samples preparation, data curation; V. N. Orlov: methodology & writing; B. B. Berezin: samples analysis, software, resources & original graft supporting; V. E. Tikhonov: conceptualization, supervision & editing; Y. A. Antonov: methodology, reviewing, writing & validation.

Conflict of interest

The authors declare that they have no competing financial interests or personal relationships that could have appeared to influence the work reported in this paper.

References

[1] Wijesinghe, W. A. J. P.; Wedamulla, N. E. Application of polysaccharides in food technology: A Review. *Trends Carbohydr. Res.* **2023,** *13*(2), 35-49.

[2] Ding, S.; Zhang, N.; Lyu, Z.; Zhu, W.; Chang, Y.-C.; Hu, X.; Du, D.; Lin, Y. Protein-based nanomaterials and nanosystems for biomedical applications: A review. *Mater. Today* **2021,** *43*, 166-184. https://doi.org/10.1016/j.mattod.2020.11.015.

[3] Jones, D. J.; McClements, O. G. Functional biopolymer particles: design, fabrication, and applications. *Compr. Rev. Food Sci. Food Saf.* **2010,** *9*, 374-397. https://doi.org/10.1111/j.1541-4337.2010.00118.x.

[4] Igual, M.; Martínez-Monzó, J. Physicochemical properties and structure changes of food products during processing. *Foods* **2022,** *11*(15), 2365. https://doi.org/10.3390/foods11152365.

[5] Nwachukwu, I. D.; Aluko, R. E. Food protein structures, functionality and product development. In *Food Proteins and Peptides: Emerging Biofunctions, Food and Biomaterial Applications*; Udenigwe, C., Ed.; Royal Society of

Chemistry, 2021. https://doi.org/10.1039/9781839163425-00001.

[6] Iqbal, M.; Tao, Y.; Xie, S.; Zhu, Y.; Chen, D.; Wang, X.; Huang, L.; Peng, D.; Sattar, A.; Shabbir, M. A. B.; Hussain, H. I.; Ahmed, S.; Yuan, Z. Aqueous two-phase system (ATPS): An overview and advances in its applications. *Biol. Proced.* **2016,** *18*, 18. https://doi.org/10.1186/s12575-016-0048-8.

[7] Moschakis, T.; Biliaderis, C. G. Biopolymer-based coacervates: Structures, functionality and applications in food products. *Curr. Opin. Colloid Interface Sci.* **2017,** *28*, 96-109. https://doi.org/10.1016/j.cocis.2017.03.006.

[8] Klassen, D. R.; Nickerson, M. T. Effect of pH on the formation of electrostatic complexes within admixtures of partially purified pea proteins (legumin and vicilin) and gum Arabic polysaccharides. *Food Res. Int.* **2012,** *46*, 167-176. https://doi.org/10.1016/j.foodres.2011.10.039.

[9] Malafaya, P.; Silva, G.; Reis, R. Natural-origin polymers as carriers and scaffolds for biomolecules and cell delivery in tissue engineering applications. *Adv. Drug Deliv. Rev.* **2007,** *9*, 207-233. https://doi.org/10.1016/j.addr.2007.03.012.

[10] Patino, J. M. R.; Pilosof, A. M. R. Protein-polysaccharide interactions at fluid interfaces. *Food Hydrocoll.* **2011,** *25*(8), 1925-1937. https://doi.org/10.1016/j.foodhyd.2011.02.023.

[11] Souza, C. J. F.; Garcia-Rojas, E. E. Effects of salt and protein concentrations on the association and dissociation of ovalbumin-pectin complexes. *Food Hydrocoll.* **2015,** *47*, 124-129. https://doi.org/10.1016/j.foodhyd.2015.01.010.

[12] Wei, Z., Huang, Q. Assembly of protein-polysaccharide complexes for delivery of bioactive ingredients: A Perspective Paper. *J Agric Food Chem.* **2019,** *67*(5), 1344-1352. https://doi.org/10.1021/acs.jafc.8b06063.

[13] Saravanan, M.; Rao, K. P. Pectin-gelatin and alginate-gelatin complex coacervation for controlled drug delivery: influence of anionic polysaccharides and drugs being encapsulated on physicochemical properties of microcapsules. *Carbohydr. Polym.* **2010,** *80*, 808-816. http://dx.doi.org/10.1016/j.carbpol.2009.12.036.

[14] Stounbjerg, L.; Vestergaard, C.; Andreasen, B.; Ipsen, R. Associative phase separation of potato protein and anionic polysaccharides. *Colloids Surf. A Physicochem. Eng. Asp.* **2019,** *566*, 104-112. http://dx.doi.org/10.1016/j.colsurfa.2019.01.012.

[15] Ghosh, A. K.; Bandyopadhyay, P. Polysaccharide-protein interactions and their relevance in food colloids. In *The Complex World of Polysaccharides*; Karunaratne, D. N., Ed.; Intechopen, 2012. http://dx.doi.org/10.5772/50561.

[16] Datta, S.; Christena, L. R.; Rajaram, Y. R. S. Enzyme immobilization: an overview on techniques and support materials. *3Biotech.* **2013,** *3*, 1-9. https://doi.org/10.1007/s13205-012-0071-7.

[17] Kayitmazer, A. B.; Seeman, D.; Minsky, B. B.; Dubin, P. L.; Xu, Y. Protein-polyelectrolyte interactions. *Soft Matter* **2013,** *9*, 2553-2583. https://doi.org/10.1039/c2sm27002a.

[18] Sing, C. E.; Perry, S. L. Recent progress in the science of complex coacervation. *Soft Matter* **2020,** *16*(12), 1-33. https://doi.org/10.1039/D0SM00001A.

[19] Gentil, L. Protein-polysaccharide interactions and aggregates in food formulations. *Curr. Opin. Colloid Interface Sci.* **2020,** *48*, 8-27. https://doi.org/10.1016/j.cocis.2020.03.002.

[20] Gao, S.; Holkar, A.; Srivastava, S. Protein-polyelectrolyte complexes and micellar assemblies. *Polymers* **2019,** *11*(7), 1097. https://doi.org/10.3390/polym11071097.

[21] Xu, A. Y.; Melton, L. D.; Ryan, T. M.; Mata, J. P.; Rekas, A.; Williams, M. A. K.; McGillivray, D. J. Effects of polysaccharide charge pattern on the microstructure of beta-lactoglobulin-pectin complex coacervates, studied by SAXS and SANS. *Food Hydrocoll.* **2018,** *77*, 952-963. http://dx.doi.org/10.1016/j.foodhyd.2017.11.045.

[22] Sperber, B. L. H. M.; Schols, H. A.; Stuart, M. A. C.; Norde, W.; Voragen, A. G. J. Influence of the overall charge and local charge density of pectin on the complex formation between pectin and beta-lactoglobulin. *Food Hydrocoll.* **2009,** *23*, 765-772. https://doi.org/10.1021/bm1010432.

[23] Antonov, Y. A.; Celus, M.; Kyomugasho, C.; Hendrickx, M.; Moldenaers, P.; Cardinaels, R. Complexation of pectins varying in overall charge with lysozyme in aqueous buffered solutions. *Food Hydrocoll.* **2019,** *94*, 268-278. https://doi.org/10.1016/j.foodhyd.2019.02.049.

[24] Antonov, Y. A.; Zhuravleva, I. L.; Celus, M.; Kyomugasho, C.; Lombardo, S.; Thielemans, W.; Hendrickx, M.; Moldenaers, P.; Cardinaels, R. Generality and specificity of the binding behaviour of lysozyme with pectin varying in local charge density and overall charge. *Food Hydrocoll.* **2020,** *99*, 105345. https://doi.org/10.1016/j.foodhyd.2019.105345.

[25] Antonov, Y. A.; Zhuravleva, I. L.; Celus, M.; Kyomugasho, C.; Lombardo, S.; Thielemans, W.; Hendrickx, M.; Moldenaers, P.; Cardinaels, R. Effect of overall charge and local charge density of pectin on the structure and thermal stability of lysozyme. *J. Therm. Anal. Calorim.* **2021,** *147*, 1-16. https://doi.org/10.1007/s10973-021-10954-5.

[26] Chen, Y.; Liu, Y.; Dong, Q.; Xu, C.; Deng, S.; Kang, Y.; Fan, M.; Li, L. Application of functionalized chitosan in food: A review. *Int. J. Biol. Macromol.* **2013,** *235*, 123716. https://doi.org/10.1016/j.ijbiomac.2023.123716.

[27] Shariatinia, Z. Pharmaceutical applications of chitosan. *Adv. Colloid Interface Sci*. **2019,** *263*, 131-194. https://doi.org/10.1016/j.cis.2018.11.008.

[28] Xiong, W.; Ren, C.; Jin, W.; Tian, J.; Wang, Y.; Shah, B. R.; Li, J.; Li, B. Ovalbumin-chitosan complex coacervation: Phase behavior, thermodynamic and rheological properties. *Food Hydrocoll*. **2016,** *61*, 895-902. https://doi.org/10.1016/j.foodhyd.2016.07.018.

[29] Leite Milião, G.; de Souza Soares, L.; Balbino, D. F.; de Almeida Alves Barbosa, E.; Costa Bressan, G.; Novaes de Carvalho Teixeira, A. V.; dos Reis Coimbra, J. S.; Basíli de Oliveira, E. pH Influence on the mechanisms of interaction between chitosan and ovalbumin: a multi-spectroscopic approach. *Food Hydrocoll*. **2022,** *123*, 107137. https://doi.org/10.1016/j.foodhyd.2021.107137.

[30] Wang, Y.-R.; Yang, Q.; Du, Y.-N.; Chen, H.-Q. Chitosan can improve the storage stability of ovalbumin fibrils at pH higher than isoelectric point. *Food Hydrocoll*. **2023,** *136*(A), 108286. https://doi.org/10.1016/j.foodhyd.2022.108286.

[31] Li, L.; Sun, X.; Zhang, H.; Dong, M.; Wang, J.; Zhao, S.; Shang, M.; Wang, X.; Zhangsun, H.; Wang, L. Amphiphilic nano-delivery system based on modified-chitosan and ovalbumin: Delivery and stability in simulated digestion. *Carbohydr. Polym*. **2022,** *294*, 119779. https://doi.org/10.1016/j.carbpol.2022.119779.

[32] Kim, S. H.; Ryu, Y. C.; Wang, H.-M. D.; Hwang, B. H. Optimally fabricated chitosan particles containing ovalbumin induced cellular and humoral immunity in immunized mice. *Biotechnol. Bioprocess Eng*. **2020,** *25*, 681-689. https://doi.org/10.1007/s12257-020-0004-y.

[33] Koppolu, B. P.; Smith, S. G.; Ravindranathan, S.; Jayanthi, S.; Kumar, T. K. S.; Zaharoff, D. A. Controlling chitosan-based encapsulation for protein and vaccine delivery. *Biomaterials* **2014,** *35*, 4382-4389. https://doi.org/10.1016/j.biomaterials.2014.01.078.

[34] Li, L.; Sun, X.; Zhang, H.; Dong, M.; Wang, J.; Zhao, S.;Shang, M.; Wang, X.; Zhangsun, H.; Wang, L. Amphiphilic nano-delivery system based on modified-chitosan and ovalbumin: Delivery and stability in simulated digestion. *Carbohydr. Polym*. **2022,** *294*, 119779. https://doi.org/10.1016/j.carbpol.2022.119779.

[35] Antonov, Y. A.; Zhuravleva, I. L.; Bezrodnykh, E. A.; Berezin, B. B.; Kulikov, S. N.; Tikhonov, V. E. Complexation of oligochitosan with sodium caseinate in alkalescent and weakly acidic media. *Carbohydr. Polym*. **2023,** *302*, 120391. https://doi.org/10.1016/j.carbpol.2022.120391.

[36] Bekale, L.; Agudelo, D.; Tajmir-Riahi, H. A. Effect of polymer molecular weight on chitosan-protein interaction. *Colloids Surf. B: Biointerfaces* **2015,** *125*, 309-317. https://doi.org/10.1016/j.colsurfb.2014.11.037.

[37] Rinaudo, M. Chitin and chitosan: Properties and applications. *Prog. Polym. Sci*. **2006,** *31*, 603-632. https://doi.org/10.1016/j.progpolymsci.2006.06.001.

[38] Aam, B. B.; Heggset, E. B.; Norberg, A. L.; Sørlie, M.; Vårum, K. M.; Eijsink, V. G. H. Production of chitooligosaccharides and their potential application in medicine. *Mar. Drugs* **2010,** *8*, 1482-1517. https://doi.org/10.3390/md8051482.

[39] Kulikov, S.; Tikhonov, V.; Blagodatskikh, I.; Bezrodnykh, E.; Lopatin, S.; Khairullin, R.; Philippova, Y.; & Abramchuk, S. Molecular weight and pH aspects of the efficacy of oligochitosan against meticillin-resistant *Staphylococcus aureus* (MRSA). *Carbohydr. Polymers* **2012,** *87*, 545-550. https://doi.org/10.1016/j.carbpol.2011.08.017.

[40] Verlee, A.; Mincke, S.; Stevens, C. V. Recent developments in antibacterial and antifungal chitosan and its derivatives. *Carbohydr. Polym*. **2017,** *164*, 268-283. https://doi.org/10.1016/j.carbpol.2017.02.001.

[41] Tikhonov, V. E.; Berezin, B. B.; Blagodatskikh, I. V.; Bezrodnykh, E. A. Oligochitosan hydrochloride: preparation and characterization. *J. Nesmeyanov Inst. Organoelem. Compd. Russ. Acad. Sci*. **2021,** *4*, 103-106. https://doi.org/10.32931/io2111a.

[42] Chae S. Y.; Jang, M.-K.; Nah, J.-W. Influence of molecular weight on oral absorption of water soluble chitosan. *J. Control. Release* **2005,** *102*, 383-394. https://doi.org/10.1016/j.jconrel.2004.10.012.

[43] Zhang, H.; Huang, X.; Sun, Y.; Xing, J.; Yamamoto, A.; Gao, Y. Absorption-improving effects of chitosan oligomers based on their mucoadhesive properties: a comparative study on the oral and pulmonary delivery of calcitonin. *Drug Deliv*. **2016,** *23*, 2419-2427. http://dx.doi.org/10.3109/10717544.2014.1002946.

[44] Kulikov, S. N.; Lisovskaya, S. A.; Zelenikhin, P. V.; Bezrodnykh, E. A.; Shakirova, D. R.; Balgodatskikh, I. V.; Tikhonov, V. E. Antifungal activity of oligochitosans (short chain chitosans) against some Candida species and clinical isolates of C. albicans: molecular weight-activity relationship. *Eur. J. Med. Chem*. **2014,** *74*, 169-178. http://dx.doi.org/10.1016/j.ejmech.2013.12.017.

[45] Blagodatskikh, I. V.; Kulikov, S. N.; Vyshivannaya, O. V.; Bezrodnykh, E. A.; Tikhonov, V. E. N-Reacetylated Oligochitosan: pH Dependence of Self-assembly Properties and Antibacterial Activity. *Biomacromolecules* **2017,** *18*(5), 1491-1498. http://dx.doi.org/10.1021/acs.biomac.7b00039.

[46] Zhang, Y.; Du, W.; Smuda, K.; Georgieva, R.; Bäumler, H.; Gao, C. Inflammatory activation of human serum albumin- or ovalbumin-modified chitosan particles to macrophages and their immune response in human whole blood. *J. Mater. Chem. B* **2018**, *6*, 3096-3106. http://dx.doi.org/10.1039/c7tb03096g.

[47] Ru, Q. M.; Wang, Y. W.; Lee, J. Y.; Ding, Y. T.; Huang, Q. R. Turbidity and rheological properties of bovine serum albumin/pectin coacervates: effect of salt concentration and initial protein/polysaccharide ratio. *Carbohydr. Polym.* **2012,** *88*, 838-846. http://dx.doi.org/10.1016/j.carbpol.2012.01.019.

[48] Ye, L.; Chen, H. Characterization of the interactions between chitosan/wheyprotein at different conditions. *Food Sci. Technol. Campinas* **2019**, *39*(1), 163-169. https://doi.org/10.1590/fst.29217.

[49] Plashchina, I. G.; Zhuravleva, I. L.; Antonov, Y. A. Phase behavior of gelatin in the presence of pectin in water-acid medium. *Polym. Bull.* **2007,** *58*, 587-596. http://dx.doi.org/10.1007/s00289-006-0691-3.

[50] Antonov, Y. A.; Moldenaers, P.; Cardinaels, R. Binding of lambda carrageenan to bovine serum albumin and non-equilibrium effects of complexation. *Food Hydrocoll.* **2022,** *126*, 107321. http://dx.doi.org/10.1016/j.foodhyd.2021.107321.

[51] Xiong, W.; Ren, C.; Tian, M.; Yang, X.; Li, J.; Li, B. Emulsion stability and dilatational viscoelasticity of ovalbumin/chitosan complexes at the oil-in-water interface. *Food Chem.* **2018,** *252*, 181-188. https://doi.org/10.1016/j. foodchem.2018.01.067.

[52] Yang, Y.; Barendregt, A.; Kamerling, J. P.; Heck, A. J. R. Analyzing protein micro-heterogeneity in chicken ovalbumin by high-resolution native mass spectrometry exposes qualitatively and semi-quantitatively 59 proteoforms. *Anal Chem.* **2013,** *85*, 12037-12045. https://doi.org/10.1021/ac403057y.

[53] Schmidt, S. I.; Cousin, F.; Huchon, C.; Boué, F.; Axelos, M. A. V. Spatial structure and composition of polysaccharide-protein complexes from small angle neutron scattering. *Biomacromolecules* **2009,** *10*, 1346-1357. https://doi.org/10.1021/bm801147j.

[54] Li, G.-Y.; Chen, Q.-H.; Su, C.-R.; Wang, H.; He, S.; Liu, J.; Nag, A.; Yuan, Y. Soy protein-polysaccharide complex coacervate under physical treatment: Effects of pH, ionic strength and polysaccharide type. *Innov. Food Sci Emerg Technol.* **2012,** *68*, 102612. https://doi.org/10.1016/j.ifset.2021.102612.

[55] Lavertu, M.; Xia, Z.; Serreqi, A. N.; Berrada, M.; Rodrigues, A.; Wang, D.; Buschmann, M. D.; Gupta, A. A validated ^{1}H NMR method for the determination of the degree of deacetylation of chitosan. *J. Pharm. Biomed. Anal.* **2003,** *32*, 1149-1158. https://doi.org/10.1016/S0731-7085(03)00155-9.